

Dynamics of Atoms Interacting Via the Radiation Field in an Optical Dipole Trap

D. N. Yanyshv^{1,*}, B. A. Grishanin¹, V. N. Zadkov¹, and D. Meschede²

¹ International Laser Center and Faculty of Physics, Moscow State University, Moscow, 119899 Russia

² Institute of Applied Physics, University of Bonn, Wegelerstrasse 8, 53115 Bonn, Germany

*e-mail: yanyshv@comsim1.msu.ru

Received December 28, 2004

Abstract—Theoretical study and computer simulation results for the stochastic dynamics of atoms localized in an optical dipole trap are presented. This dynamics is governed by the optical trap potential, cooling due to the Doppler effect, and heating due to the emission and absorption of virtual photons, i.e., due to the resonant dipole–dipole interactions (RDDI). It is shown that the RDDI becomes essential for closely spaced atoms, but the effect can be significantly improved by irradiating the atoms in the trap with an additional resonance probe laser beam. By varying both the optical dipole trap parameters and intensity of the probe laser field, the role of RDDI in the atomic dynamics in the trap is clarified in detail.

1. INTRODUCTION

Substantial progress was made over the last two decades from an understanding of the basics of quantum informatics towards developing its various applications, including quantum cryptography and quantum computing (see [1] and references therein). Some of these applications require the engineering of such atomic devices as a set of several atoms or ions localized in space for some essential portion of their functioning time, which allows for quantum engineering involving atomic states. A set of neutral atoms localized in an optical dipole trap [2] is considered to be one of the incarnations of such quantum-engineering devices.

By now, a few experimental efforts have been undertaken to localize atoms in an optical dipole trap and to control their positions in the trap by either changing the parameters of the trap [3] or by guiding them through the trap potential with the help of an optical conveyor belt [4]. In both cases, a detailed description of atomic motion in an optical dipole trap is of great importance in order to clarify the mechanisms that determine the atom dynamics.

One of the key characteristics of spatial atomic dynamics in the trap is the lifetime (or escape time) of the atoms in the trap (from the trap) under random perturbations [5]. A single atom localized in a micropotential hole of the dipole potential of the trap escapes from the micropotential hole as a result of either heating due to optical excitation or collisions with the buffer gas. We will not consider the latter mechanism in our work, as it has no fundamental character and can be, in principle, eliminated in the experiment. At the same time, interaction of atoms in the trap with an electromagnetic field is a fundamental process and needs to be considered in detail. Simple estimates show that the laser field of the beam that is used to form the optical dipole trap, which is far detuned from the atomic resonance, gives

an extremely low probability of absorbing and/or emitting photons. However, the resonant probe laser field used in experiments allows one to drastically enhance this rate and to significantly affect the atom dynamics in the trap [6].

In the case of several atoms localized in the trap, we also need to consider, in addition to the self-action resonant dipole–dipole interaction (RDDI) force acting on each separate atom in the trap, the RDDI force acting between different atoms. The RDDI force at large interatomic distances depends on the interatomic distance as $1/R$ and, for closely spaced atoms, as $1/R^3$. In a specific case in which two atoms are localized in the same microtrap, their escape could be a result of short-range RDDI, or so-called cold collisions between two closely spaced atoms [7].

Due to the fundamental character of the RDDI and its importance for the atom dynamics in the trap, it deserves a detailed investigation, which is presented in this paper. We performed a theoretical study and computer simulation of the stochastic dynamics of atoms localized in an optical dipole trap, the parameters of which were to be taken similar to those of real experiments [3, 4]. We also suggest using an additional resonant probe laser field in order to enhance the long-range RDDI and, thus, to clarify its role experimentally.

The paper is organized as follows. A model of an optical dipole trap and different sets of parameters corresponding to different experimental setups are described in Section 2. Physical models of the RDDI fluctuating forces in both short-range and long-range limits are outlined in Section 3, while the mathematical details are summarized in the Appendices. Equations for the modeling of atomic motion in the optical potential of the trap with various forces acting on the atoms, including the cooling force and RDDI forces, are described in Section 4. Preliminary estimates of the key

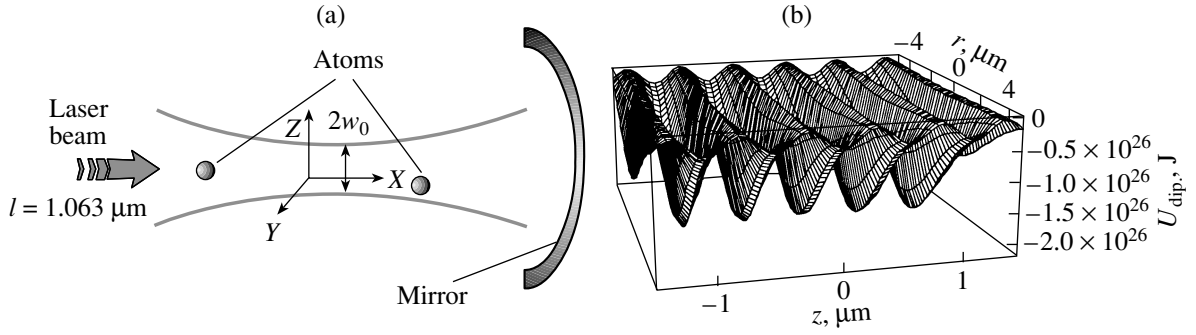


Fig. 1. Scheme of a standing-wave optical dipole trap (a) and potential energy of the trap in the radial and axial directions (b). The potential surface shows a regular pattern of micropotential holes.

parameters defining the atom dynamics, namely, the diffusion time for an atom in the trap and the escape time, which is the time that an atom needs to escape from the trap due to the RDDI, are presented in Section 5. In the computer experiments summarized in Section 6, we analyze the role of RDDI interactions affecting the dynamics of atoms in the optical dipole trap under the action of a resonant probe laser field. Varying both the parameters of the trap and the intensity and frequency detuning of the probe field, we modeled the RDDI interactions between atoms in short- and long-range limits and clarified their importance. Key results of the paper are summarized in Section 7.

2. MODEL OF AN OPTICAL DIPOLE TRAP

An optical dipole trap for neutral atoms can be made of a tightly focused powerful laser beam, the frequency of which is far detuned from the working transition of trapped atoms. One can then easily show that the interaction of the induced dipole moments of the atoms in the trap with the inhomogeneous electric field along the beam profile leads to a restoring force that “traps” the atoms inside the beam [2]. Presumably, the described trapping mechanism works only for atoms with low energies (at temperatures of about mK), because the potential of the dipole trap is shallow. Therefore, an atom should be cooled down, for example, in a magneto-optical trap, before being loaded into the optical dipole trap [3–5, 8, 9].

In experiments, for controlling the positions of atoms in the trap, it could be advantageous to keep single atoms in micropotential holes. Such a regular pattern of micropotential holes in the optical dipole trap potential can be formed using counterpropagating laser beams, which form the necessary structure due to their interference. A scheme of a standing-wave optical dipole trap formed with counterpropagating laser beams is shown in Fig. 1a. It uses only one laser beam, which interferes with the beam reflected from a mirror, thus preserving the wave front and the polarization [10]. The potential of the trap is shown in Fig. 1b.

In the following, we will consider a red-detuned optical dipole trap configuration. Such a trap is formed by a laser beam tuned far below the atomic resonance frequency. We will also assume that the laser beam with power P and wave vector k forming the trap has a Gaussian intensity profile:

$$I(r, z) = \frac{2P}{\pi w^2(z)} \exp\left(-2\frac{r^2}{w^2(z)}\right) \cos^2(kz), \quad (1)$$

where r is the radial coordinate and the half-waist beam diameter $w(z)$ depends on the axial coordinate z as

$$w(z) = w_0 \sqrt{1 + \left(\frac{z}{z_R}\right)^2}. \quad (2)$$

Here, w_0 is the beam waist diameter and $z_R = \pi w_0^2/\lambda$ is the Rayleigh length (the waist length).

As we mentioned earlier, the thermal energy $k_B T$ of atoms should be much smaller than the potential depth of the trap $U_0 = |U_{r=0, z=0}| \sim 5 \times 10^{-27}$ J and, therefore, movement of the trapped atoms in the radial direction is reasonably small compared to the beam waist diameter and, in the axial direction, the movement of the atoms is smaller than the Rayleigh length. In this case, the optical potential of the trap can be approximated as [2]

$$U_{\text{dip}}(r, z) = -U_0 \cos^2\left(\frac{2\pi}{\lambda}z\right) \left[1 - 2\left(\frac{r}{w_0}\right)^2 - \left(\frac{z}{z_R}\right)^2\right]. \quad (3)$$

From this formula, it follows that the optical potential of the trap is modulated in the axial direction with a period of $\lambda/2$. The oscillation frequencies of the trapped atoms are equal to the first approximation to $\omega_r = (4U_0/mw_0^2)^{1/2}$ in the radial and $\omega_z = k(2U_0/m)^{1/2}$ in the axial directions, respectively.

When a dipole trap contains atoms (we will consider Cs or Rb atoms, which are typically used in optical dipole trap experiments), one can also note that the potential of the trap to the next approximation depends on the energy shift of the atomic levels in the trap due

to the interaction with the off-resonant radiation. Taking this into account (and neglecting the hyperfine splitting of the levels) [2], the potential energy of the trap reads

$$U_{\text{dip}}(r, z) = -\frac{\pi c^2 \Gamma}{2\omega_0^3} \left(\frac{2}{\Delta_2} + \frac{1}{\Delta_1} \right) I(r, z), \quad (4)$$

where Δ_1 and Δ_2 are the frequency detunings of the laser radiation from the frequencies of the atomic transitions $^2S_{1/2} \longleftrightarrow ^2P_{1/2}$ and $^2S_{1/2} \longleftrightarrow ^2P_{3/2}$, respectively; Γ is the natural linewidth; and ω_0 is the resonance atomic transition frequency.

An additional resonant laser probe field that can be used in experiments with trapped atoms in the optical dipole trap modifies not only the radiation processes but also the optical potential of the trap due to redistribution of the population from the ground energy level of the atoms. As a result, the optical potential is reduced:

$$U_{\text{dip}}(r, z) = -\frac{(n_1 - n_2)\pi c^2 \Gamma}{2\omega_0^3} \frac{2P}{\pi w^2(z)} \left(\frac{2}{\Delta_2} + \frac{1}{\Delta_1} \right) \times \exp\left[-2\frac{r^2}{w^2(z)}\right] \cos^2(kz), \quad (5)$$

where

$$(n_1 - n_2) = 1 - \frac{2\tilde{g}_l^2}{(1 + \tilde{\delta}^2 + 2\tilde{g}_l^2)}$$

is the population difference of the lower and upper atomic levels and $\tilde{\delta} = \Delta/\Gamma$ and $\tilde{g}_l = \Omega_R/\Gamma = dE/\hbar\Gamma$ are the dimensionless frequency detuning and the Rabi frequency, which both depend on the probe field intensity.

The parameters of the optical dipole trap that we used in our model for numerical simulations throughout the paper have been taken to be similar to the parameters of the experimental setups of [3, 5].

Specifically, in [5], the optical dipole trap is formed by focusing a 2.5-W Nd:YAG laser beam (1.064 μm) with linear polarization along the x axis into an area with a diameter of about 5 μm . Cesium atoms (working transitions at 852 and 894 nm) trapped in the optical dipole trap are assumed to be two-level atoms with excited-state lifetimes of $1/\gamma = 3.07 \times 10^{-8}$ s, and the dipole moment of the working transition is $d = 8.01 \times 10^{-18}$ SGSE. The frequencies of the atomic oscillations in the radial and axial directions are equal to $\omega_r \approx 60$ Hz and $\omega_z \approx 1.5$ MHz, respectively.

In [3], the optical dipole trap is formed by strong focusing of a 3-mW laser beam at 810 nm into a waist ~ 1 μm diameter, which allows for deep localization of atoms in the micropotential holes. Rubidium atoms (working transitions at 780 and 795 nm) are used in the experiment.

3. MODELING OF THE RESONANT DIPOLE–DIPOLE INTERACTIONS OF ATOMS

In this section, we will consider how to model the resonant dipole–dipole interaction (RDDI) of atoms in the trap, which can significantly affect the atomic dynamics in the trap and result in the escape of atoms from the trap [7, 11]. In our approach, we will distinguish between long-range and short-range RDDI, which drastically differ in typical interaction energy and timescale. This will allow us to use qualitatively different models for these types of RDDI—an adequate model for the long-range RDDI is the white noise process, which leads to diffusion-type motion of atoms in the trap, whereas the short-range RDDI can be modeled well with a pulse train–like process, which results in spasmodic motion of the atoms in the trap. Both of these processes, however, are considered in the Markov approximation, which is valid because the respective correlation times of the processes are much smaller than the typical dynamical changes in the considered system.

The mathematical details are summarized in the Appendices, whereas below we outline the physical models that are used for further computer simulations.

3.1. Modeling of the Long-Range RDDI Force

In order to describe the radiation force acting on the atoms, we will consider the electromagnetic field acting on the atoms and the quantum fluctuations due to the virtual photon exchange [12]. The quantum nature of the fluctuations is taken into account after the elimination of a virtual photon by the operator character of the corresponding fluctuating interaction force, which is equally replaced with the classical white noise, whose nonzero average value is defined versus the parameters of the exciting laser field causing either Doppler cooling or heating [13]. In this model, both the self-action of an atom due to the reemission of a photon and the interaction of two atoms via the exchange of virtual photons are described equally well with the same correlation matrix of the fluctuation force (see Appendices).

With the assumptions made above, we can calculate the spectrum of the atomic radiation force, which, for the case of a single atom that reemits the photons (self-action force), is described by the 3D-vector of the random force \mathbf{F}_i acting on the i th atom (see Appendix B, Eq. (B3)):

$$N_{ii} = \frac{\hbar\omega_0^5 d^2}{2\pi c^5} \langle \Delta\sigma_1^- \Delta\sigma_1^+ \rangle I_{11}, \quad (6)$$

where I_{11} is the 3×3 matrix composed of numerical constants, $d = (3\hbar c^3 \Gamma / 4\omega_0^3)^{1/2}$ is the atomic transition dipole moment, and $\hat{\sigma}_\pm$ are the atomic transition operators.

For two atoms (i and k) interacting via the long-range RDDI, the spectral matrices of the fluctuation force have, according to Appendix C, the form (see Eq. (C6))

$$N_{ik} = N_{ki} = \frac{\hbar \omega_0^5 d^2}{2\pi c^5} \langle \Delta \sigma_1^- \Delta \sigma_2^+ \rangle I_{12}, \quad (7)$$

where I_{12} is the dimensionless 3×3 matrix that is determined by the geometry of the atomic dipole moments with respect to the vector of the dipole moment displacement and to the vector of an emitted photon. For the dipole moments parallel to each other and orthogonal to the vector of displacement and to the vector of the emitted photon, we have

$$I_{11} = \pi \begin{pmatrix} \frac{8}{15} & 0 & 0 \\ 0 & \frac{16}{15} & 0 \\ 0 & 0 & \frac{16}{15} \end{pmatrix}, \quad I_{12} = \pi \begin{pmatrix} \tilde{I}_1 & 0 & 0 \\ 0 & \tilde{I}_2 & 0 \\ 0 & 0 & \tilde{I}_3 \end{pmatrix}, \quad (8)$$

where

$$\langle \Delta \sigma_1^- \Delta \sigma_2^+ \rangle = \frac{-4g\tilde{g}_L^4(1+4\delta^2)}{[(1+g)^2 + 4(\tilde{g}_L^2 + \delta^2) + 4(1+g)^2\delta^2 + 4(\tilde{g}_L^2 + 2\delta^2)^2]^2},$$

where $\tilde{g}_L = g_L/\Gamma$ is the dimensionless Rabi frequency; $g_L = Ed/\hbar$ is the Rabi frequency; $\delta = \Delta/\Gamma$ is the dimensionless probe laser frequency detuning; and

$$g = \frac{3\varphi \cos \varphi - \sin \varphi + \varphi^2 \sin \varphi}{\varphi^3}$$

is the dimensionless geometrical factor, which, for interatomic distances $R_{12} > \lambda$, is simplified to $g = 3 \sin \varphi / 2\varphi$.

It is clear that, if we reduce the interatomic distance to zero, $\lim_{\varphi_{12} \rightarrow 0} I_{12} = I_{11}$, we will obtain the fluctuations of a single atom. Therefore, assuming $g = 1$, we can calculate the correlation function of the fluctuations of a single atom, which reads

$$\begin{aligned} & \langle \Delta \sigma_1^- \Delta \sigma_2^+ \rangle \\ &= \frac{2\tilde{g}_L^4(1 + 2(\tilde{g}_L^2 + \delta^2) + (1 + 4\delta^2))}{(4 + 4(\tilde{g}_L^2 + \delta^2) + 16\delta^2 + 4(\tilde{g}_L^2 + 2\delta^2)^2)}. \end{aligned}$$

$$\begin{aligned} \tilde{I}_1 &= \frac{4(9 - \varphi_{12}^2) \cos \varphi_{12}}{\varphi_{12}^4} - \frac{4(9 - 4\varphi_{12}^2) \sin \varphi_{12}}{\varphi_{12}^5}, \\ \tilde{I}_2 &= \frac{4(3 - \varphi_{12}^2) \cos \varphi_{12}}{\varphi_{12}^4} - \frac{4(3 - 2\varphi_{12}^2) \sin \varphi_{12}}{\varphi_{12}^5}, \\ \tilde{I}_3 &= \frac{-4(12 - 3\varphi_{12}^2) \cos \varphi_{12}}{\varphi_{12}^4} \\ &+ \frac{4(9 - 12\varphi_{12}^2 + \varphi_{12}^4) \sin \varphi_{12}}{\varphi_{12}^5}. \end{aligned} \quad (9)$$

and $\varphi_{12} = R_{12}\omega_0/c$ is the dimensionless interatomic distance.

From Eqs. 9, one can easily see that, at $R_{12} \rightarrow 0$, the coefficients $\tilde{I}_{1,2,3}$ grade into the respective coefficients for a single atom $\tilde{I}_2 = \tilde{I}_3 = 2\tilde{I}_1 = 16/15$. At large interatomic distances, i.e., at $R \gg \lambda$, Eqs. 9 can be approximated by $\tilde{I}_1 = \tilde{I}_2 = 0$, $\tilde{I}_3 = 4 \sin \varphi_{12} / \varphi_{12}$.

In Eqs. (6) and (7), $\langle \Delta \sigma_1^- \Delta \sigma_2^+ \rangle$ is the correlation function of the operator of photon exchange between two atoms, which reads

From Fig. 2b, one can clearly see that the correlation function of the photon-exchange operator between two atoms, $\langle \Delta \sigma_1^- \Delta \sigma_2^+ \rangle$, which describes the interaction between the atoms, reaches its maximum at the detuning $\delta = -1$, when the interaction force between atoms has its maximum value with respect to the fluctuation of the self-acting force for a single atom. Such a maximum is reached at $g_L = 1.4$, which corresponds to the probe laser intensity $I = 7.1 \text{ W/cm}^2$.

3.2. Modeling of the Short-Range RDDI Force

At short interatomic distances that correspond, for instance, to the case of two atoms in the same micropotential hole in the optical dipole trap, we need to consider the system of “two atoms plus the electromagnetic field” or the following process: $A + A + \hbar\omega \rightarrow A_2^*$ [7]. Below, we outline how this process can be modeled.

Let us first note that, during absorption or emission of a photon, an essential part of the photon’s energy $\hbar\omega_0 \sim 10^4 \text{ K}$ is transferred into the translational degrees of freedom of the atom that is absorbing or emitting the

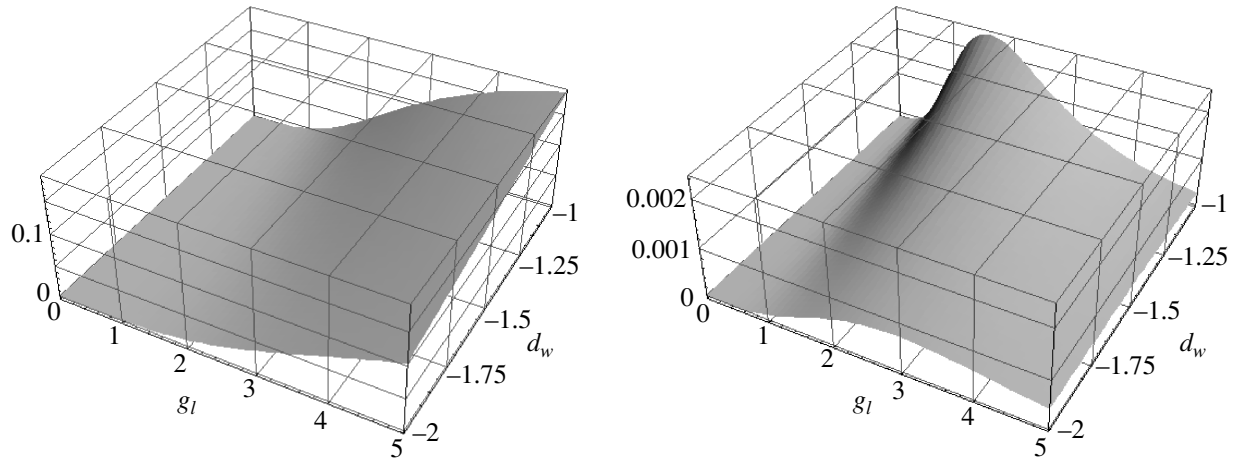


Fig. 2. Correlation functions of the fluctuations of a single atom, $\langle \Delta\sigma_1^- \Delta\sigma_1^+ \rangle$ (a), and the operator of photon exchange photons between two atoms, $\langle \Delta\sigma_1^- \Delta\sigma_2^+ \rangle$ (b), versus the dimensionless laser detuning δ and the Rabi frequency g_L .

photon. This could result in the escape of the atom from the micropotential hole and then from the trap. The probability of this process depends on the intensity of the probe resonant/near-resonant laser field, its frequency detuning from the atomic resonance, and the interatomic distance. (Note also that the interaction of closely spaced atoms can compensate for even a large detuning of the incident laser field.)

Then, let us assume that the interaction potential between closely spaced atoms can be described with the following simple dependence:

$$\Delta U(R_{12}) = C/R_{12}^6,$$

where $C = \text{Const}$ and R_{12} is the interatomic distance. Then, we can approximate the atomic frequency shift due to the quasi-electrostatic dipole-dipole interaction of atoms with respect to the laser field intensity as follows:

$$\delta(t) = \Delta + \delta_0(a_0/R_{12})^6,$$

where Δ is the frequency detuning of the laser field forming the optical dipole trap, $\delta_0 = 10^{12}$ is the parameter that defines the frequency shift due to the interaction of atoms, and $a_0 = 1$ nm is the Weisskopf radius [14].

The corresponding Hamiltonian, which describes the modified interaction with the field at a given frequency detuning, can be written as

$$\hat{H}(t) = \frac{\hbar\delta(t)}{2}\hat{\sigma}_3 + \frac{\hbar\Omega_0}{2} \begin{pmatrix} 0 & 1 \\ 1 & 0 \end{pmatrix},$$

where Ω_0 is the Rabi frequency. Then, in the adiabatic approximation, the corresponding population of the

upper level can be written as

$$n_2(t) = \frac{\Omega_0^2}{\Omega_0^2 + \delta^2(t)} \sin^2 \left(\frac{\sqrt{\Omega_0^2 + \delta^2(t)}}{2} t \right).$$

Keeping in mind that the time between atomic collisions $\tau_{\text{coll}} = a_0/V \approx 10^{-9}$ s significantly exceeds the Rabi oscillation period $\tau_0 \approx 10^{-11}$ s, we can average the above formula over the period τ_0 , which results in the following population of the upper level:

$$n_2(t) = \frac{1}{2} \frac{\Omega_0^2}{\Omega_0^2 + \delta^2(t)}, \quad (10)$$

which determines, within the frame of our approximations, the probability for an atom to leave the trap due to a cold collision.

One can see from Eq. (10) that, at $\delta \rightarrow 0$ (and, respectively, at $R_{12} \rightarrow a_0(\delta_0/\Delta\omega)^{1/6}$), the probability for an atom to leave the trap reaches its maximum and is equal to 1/2. This means that, while modeling the cold collisions, one should take into account how the cold-collision probability depends on the interatomic distance.

4. MODELING OF ATOMIC MOTION IN THE TRAP

The motion of atoms in the trap is governed by the following equation:

$$m\ddot{\mathbf{r}}^{(i)} = -\frac{\partial U_{\text{dip}}^{(i)}}{\partial \mathbf{r}^{(i)}} + \mathbf{F}_{\text{cool}}^{(i)} + \sum_j \mathbf{F}_{\text{RDDI}}^{(i,j)}, \quad i, j = 1, 2 \quad (11)$$

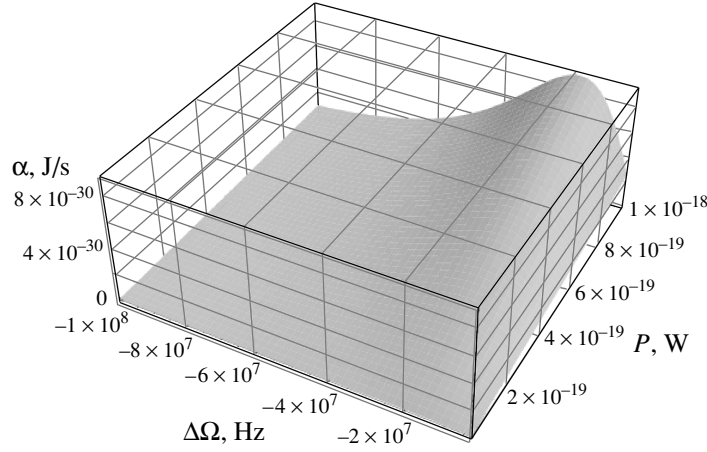


Fig. 3. Radiation friction coefficient α versus the dimensionless frequency detuning $2\delta/\gamma_0$ and the normalized probe laser beam intensity I/I_0 .

where the indices i and j number atoms in the trap, U_{dip} is the optical potential of the trap (see Section 2), \mathbf{F}_{cool} is the cooling force (linear friction), and $\mathbf{F}_{\text{RDDI}}^{(i,j)}$ is the fluctuation force due to the RDDI. If $i = j$, the RDDI force corresponds to the case of the RDDI self-action force for the atom itself; otherwise, it is the RDDI force between two interacting atoms (see Section 3).

The cooling force due to the Doppler effect can be written as [13]

$$\mathbf{F}_{\text{cool}} = -m\alpha\dot{\mathbf{r}}_z, \quad (12)$$

where

$$\alpha = -\frac{2\hbar\omega^2 I}{mc^2 I_0 [1 + (2\delta/\gamma_0)^2]^2}$$

is the radiation friction coefficient (plotted in Fig. 3), I is the near-resonant probe laser beam intensity, and I_0 is the saturation intensity of the atomic transition.

The fluctuation RDDI force \mathbf{F}_{RDDI} can be modeled with the help of equations derived in Section 3 for the cases of both long- and short-range RDDI. While modeling the dynamics of closely spaced atom in the trap (for instance, atoms located in the same micropotential hole), the latter leads to the so-called cold collisions and, as a result, to the escape of atoms from the trap.

In order to simulate the fluctuating character of the RDDI forces on a computer, we model it with the help of independent random forces, the amplitudes of which are generated with the help of a computerized random-number generator in such a way so as to preserve the given level of the mean-square fluctuations of the RDDI forces. Specifically, we use the following formula for the mean-square dispersion of the integral of

the RDDI force acting on an atom or atoms over the sampling time Δt :

$$\sigma_{\lambda}^{ij^2}(\Delta t) = \left[\int_0^{\Delta t} F_{\lambda}^{ij}(\tau) d\tau \right]^2 = N_{\lambda}^{ij} \Delta t, \quad (13)$$

where $F_{\lambda}^{(i,j)}$ are the projections on the axes $\lambda = x, y, z$ of the fluctuation force $\mathbf{F}^{(i,j)}$; $N_{\lambda}^{(i,j)}$ are the nonzero components of the spectral density matrix N calculated with the help of Eqs. (6) and (7); $N_{\lambda}^{(i,j)}$ describe the diagonal elements of the 3×3 submatrices of the block matrix of the form

$$N = \begin{pmatrix} N^{11} & -N^{12} \\ -N^{12} & N^{11} \end{pmatrix};$$

and i, j label the atoms. Projections of the forces $F_{f\lambda}^{(i)} = \sum_j \mathbf{F}^{(i,j)}$, which satisfy relation (13), can be written with the help of independent random variables as

$$\begin{aligned} F_{f\lambda}^{(1)} &= (\sqrt{2(N_{\lambda}^{11} + N_{\lambda}^{12})/\Delta t} \xi_1^{\lambda} \\ &\quad - \sqrt{12(N_{\lambda}^{11} - N_{\lambda}^{12})/\Delta t} \xi_2^{\lambda}) / \sqrt{2}, \\ F_{f\lambda}^{(2)} &= (\sqrt{12(N_{\lambda}^{11} + N_{\lambda}^{12})/\Delta t} \xi_1^{\lambda} \\ &\quad + \sqrt{12(N_{\lambda}^{11} - N_{\lambda}^{12})/\Delta t} \xi_2^{\lambda}) / \sqrt{2}, \end{aligned} \quad (14)$$

where $\xi_{1,2}^{\lambda}$ are the independent random variables uniformly distributed in the interval $[-1/2, 1/2]$, which can be generated with the help of a regular computerized random-number generator.

5. PRELIMINARY ESTIMATES

Before we discuss simulation results for the atomic motion in the trap in the next section of the paper, let us first make some estimates of the key parameters defining atomic dynamics, namely, the diffusion time for an atom in the trap and the escape time, which is the time an atom needs to escape from the trap due to the RDDI (in the next section, all other factors are also taken into account).

The typical energy that an atom receives from the recoil after photon emission or absorption can be estimated with the help of the following formula:

$$\varepsilon = -(\hbar\omega/c)^2/2mk_B \approx 0.2 \text{ } \mu\text{K}.$$

It does not exceed the potential microtrap depth, which is of the order of 16 mK [5]. Therefore, the absorption or emission of single photons does not lead to the atom's escape from the microtrap, and we can model the atomic motion as a diffusion process. The typical diffusion time for such a process, $T \sim 10^{-8}$ s, is much smaller than all of the typical times of the translational atomic motion in the trap, so that the Markov approach is adequate for use.

Let us first estimate the typical time necessary for atoms to escape from the trap due to the action of the probe resonant laser field but without the optical potential of the trap. In this case, the dynamics of an atom in the trap can be considered in velocity space as the Wiener process, which is characterized by the linear growth of the atom's velocity dispersion versus time, and we can estimate the escape time of the atom as

$$\tau_f = \sqrt[3]{\frac{m_a^2 a^2}{N_0}}, \quad (15)$$

where m_a is the atom mass, a is the typical size of the trap, and N_0 is the spectrum of the fluctuating force. Putting the experimental parameters given in Section 2 into Eq. (15), we get $\tau_f \sim 10^{-4}$ s.

Then, let us estimate the typical diffusion time for an atom in the trap assuming that the atom undergoes a "narrow-band dynamics," when the spectrum of atom oscillations is localized in the vicinity of the fundamental frequency ω_0 . This assumption is valid because the atomic oscillations are much faster than the time necessary for the atom to leave the trap due to the fluctuating RDDI force. Therefore, the narrow-band dynamics regime is established. In this regime, oscillations of atoms have the following form:

$$x(t) = x_c(t) \cos \omega_0 t + x_s(t) \sin \omega_0 t,$$

where x_c and x_s describe slow (with respect to the carrier frequency) independent oscillations of the quadrature amplitudes. Instead of exact second-order equa-

tions for these quadratures, in our case, we can use the shortened equations of the form

$$m_a \omega_0 \frac{dx_c}{dt} + m \alpha \omega_0 x_c = \xi(t). \quad (16)$$

In order to estimate the diffusion time, one needs to neglect the friction α . Then, the solution is simply the integral of $\xi(t)$ over the time, and averaging over its quadrature gives

$$\langle \Delta x^2 \rangle = \frac{N_0 \Delta t}{m_a^2 \omega_0^2}.$$

Replacing Δx with the typical size of the microtrap a , we will get the typical diffusion time Δt :

$$\tau_D = \frac{m_a^2 \omega_0^2 a^2}{N_0} \sim 10^{-2} \text{ s}. \quad (17)$$

Though the estimates we made in this section are relatively rough, they fulfill the validity relation $\tau_D \gg 2\pi/\omega_0$ between the diffusion time and the period of atomic oscillations. Comparing the diffusion time with the friction parameters of the trap, one can make preliminary conclusions about the probability of atoms escaping from the trap due to the fluctuating RDDI force.

6. COMPUTER SIMULATION RESULTS OF ATOM DYNAMICS IN AN OPTICAL DIPOLE TRAP

In computer experiments summarized in this section, we analyze the role of the RDDI interactions affecting the dynamics of atoms in an optical dipole trap under the action of a resonant probe laser field. Varying both the parameters of the trap and the intensity and frequency detuning of the probe field, we were able to model the RDDI interactions between atoms in short- and long-range limits and to clarify their importance. The influence of a buffer gas in the trap has not been taken into account in our model.

The motion of atoms in the trap is calculated with the help of Eq. (11). In modeling the trajectories of atoms, we set the initial coordinates of the atoms as random deviations from the equilibrium coordinates in the minima of the optical potential of the trap, and their initial velocities are distributed according to the Maxwell distribution at a given temperature. The latter depends on the temperature of the atoms, which we set equal to the experimental value of about $T = 40 \text{ } \mu\text{K}$ [3–5]. At this temperature, atoms are localized in the micropotential minima for quite a long time.

By varying the intensity of the resonant probe laser field, we can vary the degree of the RDDI interaction of atoms in the trap and, correspondingly, the lifetime of the atoms in the trap. As follows from Fig. 2b, the maximum fluctuating RDDI force is achieved at the maximum of the correlation function in the figure, i.e., at an

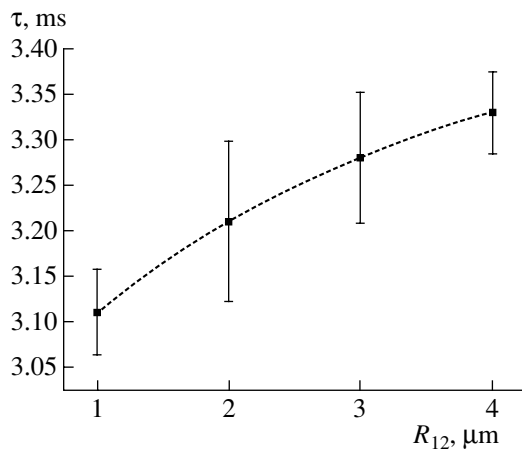


Fig. 4. Lifetime of atoms in an optical dipole trap versus the interatomic distance at $I/I_0 = 3$.

intensity of the resonant probe laser beam of about 0.071 W/cm^2 (Section 3A).

By also varying the interatomic distance, we can study how the atom dynamics depends on the distance between potential microholes of the optical dipole potential in which the atoms are localized. The qualitative difference between the case of two atoms localized in different/neighboring microtraps and in the same microtrap is that, in the former case, there are no cold collisions between atoms.

In our computer experiment, we will first study the case of a tightly focused optical dipole trap with the parameters found in [3], which provides for deep localization of atoms in the microtraps. As a result, we have strong RDDI interaction between atoms localized in the same microtrap and, correspondingly, a short lifetime of atoms in the trap. Experimental conditions also allow for the interatomic distance to be changed between 1 to $10 \mu\text{m}$, which covers both the case of two atoms in the same microtrap or of two atoms in different microtraps that we simulate in the computer experiments.

Computer simulation results for the lifetime of atoms in the optical dipole trap versus the interatomic distance are shown in Fig. 4. These results show that the lifetime of atoms in the trap increases with increasing interatomic distance, which means that the RDDI interaction between atoms under the action of the resonance probe laser field vanishes for large interatomic distances. The lifetime dependence in Fig. 4 can be approximated with the following simple exponential expression:

$$\tau = -4.80 \times 10^{-4} e^{-R/2.87} + 3.45 \times 10^{-3} \text{ s}, \quad (18)$$

where R is the average over the atom's oscillatory interatomic distance in μm . It is important to note here that our simulation results for the lifetime correspond well to our previous estimate of the diffusion time in Section 5.

Due to the fluctuating character of the RDDI force, our simulation results also have statistical character and must be averaged over a large number of realizations in order to give reliable numbers. The dependence in Fig. 4 clearly shows a substantial dispersion, which is due to the small number of computed realizations (ten in our case).

From numerical simulation of Eqs. (11), we can estimate, for the case of long-range RDDI, the heating rate of atoms in the trap under the action of the resonance probe laser field with the help of the following approximate formula:

$$\frac{\Delta E}{\Delta t} = 7.57 \times 10^{-23} - 1.18 \times 10^{-23} e^{-(R/2.53)} \text{ J/s}, \quad (19)$$

where R is the average interatomic distance in μm over the atomic oscillations.

In order to estimate how essential the contribution from the fluctuating RDDI force due to the interactions between atoms is, we need to make similar calculations under the same conditions for a single atom. This gives us an average lifetime (or escape time) of the atom in the microtrap of $\tau = 4.05 \times 10^{-3} \text{ s}$ and, respectively, a heating rate

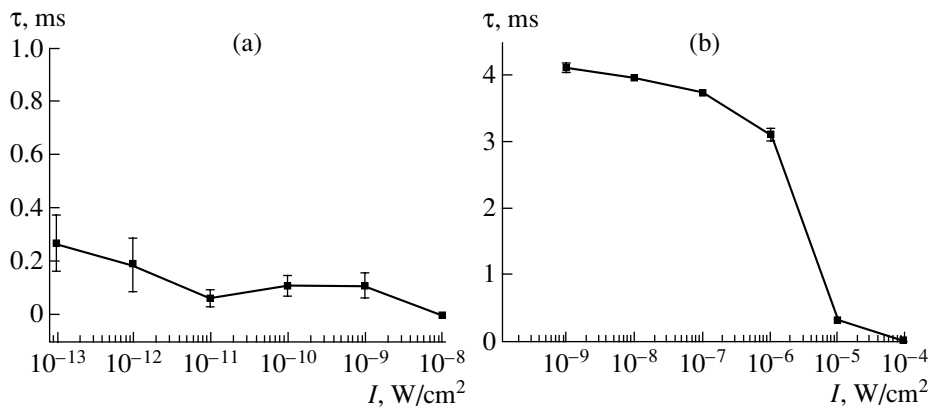
$$\frac{\Delta E}{\Delta t} = 6.42 \times 10^{-23} \text{ J/s}. \quad (20)$$

Comparing this result with the previous one for two interacting atoms, one can clearly see that the RDDI force between two atoms gives a substantial contribution when atoms are spaced by a distance of approximately equal to or less than the wavelength; with increasing interatomic distance, the force rapidly vanishes and the self-action RDDI force dominates (see Section 3).

One can also check if the dynamics of a single atom in the trap is similar to the dynamics of one of the two atoms in the trap when the interatomic distance between them significantly exceeds the wavelength (in the limit $R \rightarrow \infty$). This can be easily done both by comparing approximating formulas (19) and (20) and

by a special numerical simulation, which gives $\frac{\Delta E}{\Delta t} = 6.39 \times 10^{-23} \text{ J/s}$, a value that corresponds well with estimate (20) for the heating rate of a single atom in the trap.

In case in which both atoms are located in the same microtrap, the short-range RDDI could lead to cold collisions between them and, finally, in the escape of an atom or atoms from the trap. At a resonant probe laser field intensity that is lower than the saturation intensity of the atom, these cold collisions practically do not depend on the resonant field intensity and can be described by a jump process of atoms escaping from the trap [3]. When the intensity of the resonant probe laser field is of the same order of magnitude as the saturation intensity or exceeds it, the short-range RDDI comes



1 **Fig. 5.** Lifetime dependencies of two atoms in the trap, which sit either in one (a) or in neighboring (b) micropotential holes versus the resonance laser pump intensity.

into play and results in a substantial reduction of the escape time for atoms in the trap, up to the case when the probability of an atom escaping from a microtrap populated by two atoms becomes equal to the probability of single atoms escaping from different microtraps.

Simulation results for the lifetime of atom(s) in the trap at moderate intensities are shown in Fig. 5. An analysis of the results for two atoms sitting in one microtrap (shown in Fig. 5a) give the following estimate for the average lifetime:

$$\tau(g_l) = 1.48 \times 10^{-4} \text{ s},$$

where $g_l \ll 1$ is the dimensionless Rabi frequency. Though the lifetime is a constant, its estimate (as can be seen in Fig. 5) has an essential dispersion. Our simulation results correspond well to those of an experiment with atoms in an optical dipole trap [3] (for the parameters of the experiment, see also Section 2).

With the different set of experimental parameters used in [5], the atoms in the trap are much less well-localized in the radial direction and the localization area is about $\sim 5 \mu\text{m}$. As a result, we can expect cold collisions with a probability two orders of magnitude less than for the previous set of parameters. From a simple formula for the collision frequency

$$\nu = \sigma v / V,$$

where σ is the collision cross section, v is the average atom velocity, and V is the volume where atoms are localized, it follows that increasing the localization volume results in a decrease in the collision frequency. Even such a simple estimate shows that, for these experimental conditions, we predominantly have the case of diffusion-type motion of the atoms in the trap, even in the case when both atoms are localized in the same microtrap.

Additional information in the computer simulation results lies in the spectrum of the dynamical variables of atoms localized in the trap. Equation (11), which governs the motion of atoms in the trap, is a nonlinear

equation, and the oscillations of the atoms are quasi-harmonic. Therefore, a decrease in the frequency of atomic oscillations (i.e., the low-frequency shift of the spectrum of oscillations) due to the anharmonicity of the oscillation potential as a function of amplitude gives us additional information about an increase in the amplitude of the oscillations and, respectively, the energy of an atom. Spectra of the oscillations of a single atom and one of the two interacting atoms in the trap are shown in Fig. 6.

Also, the width of the spectrum of atomic oscillations characterizes how the resonant probe laser radiation affects the fluctuations of the atoms due to the RDDI. An increase in the RDDI fluctuating force leads to deformation of the spectrum (it is shifted in frequency and becomes wider), which is absent at small atomic energies ($E = kT \ll U_{\text{dip}}$), when the harmonic

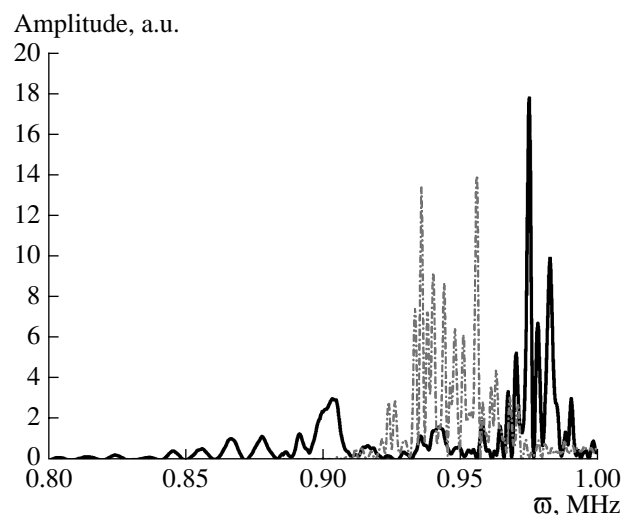


Fig. 6. Spectra of oscillations of a single atom (solid line) and one of the two interacting atoms in the trap (dashed line) along the z axis at $I/I_0 = 3$.

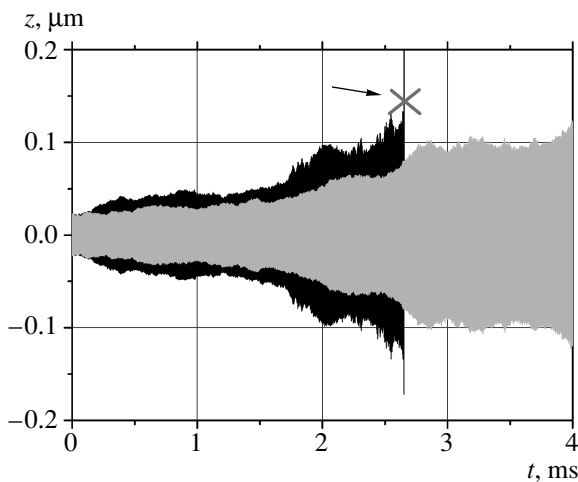


Fig. 7. Temporal dependence of the axial coordinate of a single atom (solid line) and the center of gravity of two interacting atoms (dashed line) in the trap with the same initial conditions at $I/I_0 = 3$. The symbol \times denotes the moment when the atom leaves the trap.

approximation we used in Section 2 to estimate the oscillation frequency of atoms in the microtraps is valid.

Because the RDDI interaction for a single atom and two interacting atoms in the trap leads qualitatively to the effective heating of atom(s) and, therefore, allows them to escape from the trap, it is worthwhile to make a comparative analysis of a single atom and one of the two interacting atoms in the trap at the same initial conditions. Such simulation results are shown in Figs. 7 and 8.

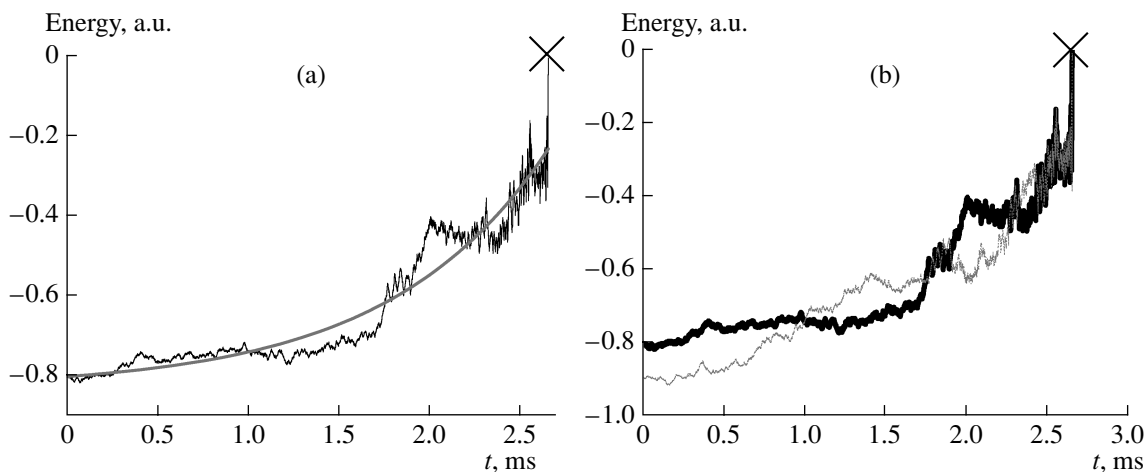


Fig. 8. (a) Temporal dependence of the total energy of a single atom in a micropotential hole and its theoretical approximation (smooth solid line). (b) Temporal dependencies of the total energies of a single atom in the trap (solid line, similar to (a)) and one of the two atoms trapped in neighboring micropotential holes at the resonance laser pump intensity $I = 3I_0$, where I_0 is the resonance transition saturation intensity. The symbol \times denotes the moment when the atom leaves the trap.

From Fig. 8, we can estimate the lifetime of the atom in the trap versus its initial energy, which can be approximated with the following exponential dependence:

$$\tau = 2.33 \times 10^{-3} e^{-E/0.173U_0} \text{ s.}$$

Figure 8b shows the temporal dependencies of the total energies of a single atom in the trap and one of the two atoms trapped in neighboring micropotential holes. One can clearly see that, by the end of the time scale, the total energy of the atoms has sharply increased in value, which indicates that the atoms leave the trap at this moment. An analysis of both Figs. 8a and 8b shows that the RDDI can result in atoms escaping from the microtrap in both cases—when a single atom sits in a microtrap and when two atoms sit in the same or neighboring microtraps.

7. CONCLUSIONS

In conclusion, we have theoretically and in computer simulations clarified the role of resonant dipole-dipole interactions on the atom dynamics in an optical dipole trap under the action of an additional resonant probe laser field. It is shown that the interaction of atoms via the RDDI causes a substantial modification of the atom dynamics and a shortening of the lifetime of the atoms in the trap. Due to its physical nature, the RDDI is observed more clearly in the case of closely spaced atoms, for instance, atoms localized in the same micropotential hole of the optical potential of the trap. However, this effect can be significantly increased by irradiating atoms localized in the trap with an additional resonant probe laser beam. By varying both the parameters of the optical dipole trap and the intensity of

the probe field, we can study the role of short- and long-range RDDI on atoms in the trap in detail.

The results of the computer simulations that we performed for two different sets of parameters of the optical dipole trap, which correspond to different experimental realizations [3, 4], fit the experimental data well. Both the theoretical estimates and the computer simulations prove that the RDDI can result in the escape of atoms from the trap and can reduce the lifetime of the atoms in the trap.

ACKNOWLEDGMENTS

This work was partially supported by the Russian Foundation for Basic Research, grant no. 04-02-17554, and INTAS, grant INFO 00-479.

APPENDIX A

QUASI-CLASSICAL MODEL FOR THE RDDI

There are two key approaches to modeling the radiation force fluctuations, namely, classical and quantum [11]. Despite certain limitations of the classical approach, it is used in many applications, especially for calculation of the statistical properties of the fluctuating

forces. The latter is valid until the responding quantum representation of the force can be written in a classical-like form $\hat{\mathbf{F}} = \nabla \hat{\mathbf{d}} \hat{\mathbf{E}}_0$ without any substantial loss of the key peculiarities of the problem [15]. Here, $\hat{\mathbf{d}}$ and $\hat{\mathbf{E}}_0$ are the operators of the atomic dipole moment and the vacuum electric field, respectively. In accordance with [12], let us assume that the fluctuating force can be treated as external white noise. Then, all the information on $\hat{\mathbf{F}}$ that is interesting to us can be described in terms of the correlation function for two atoms at the points $\hat{\mathbf{R}}_\mu$ and $\hat{\mathbf{R}}_\nu$:

$$G_{\mu\nu}(\tau) = \langle \hat{\mathbf{F}}(\hat{\mathbf{R}}_\mu, 0) \hat{\mathbf{F}}^T(\hat{\mathbf{R}}_\nu, \tau) \rangle, \quad (\text{A1})$$

where the angle brackets denote averaging over both the field and the internal atomic fluctuations; the superscript T denotes vector transposition and transforms the column vector $\hat{\mathbf{F}}$ into a corresponding row, so that $G_{\mu\nu}$ for the fixed values μ , where ν is a 3×3 matrix.

From Eq. (A1), because of space delocalization of the dipole moment and with the help of the diffusion Markovian approach for the translational atomic dynamics, we get

$$G_{\mu\nu}(\tau) = \iint \left\langle \frac{\partial}{\partial \mathbf{R}_\mu} \hat{\mathbf{d}}^T(\mathbf{r} - \hat{\mathbf{R}}_\mu, 0) D(\mathbf{r} - \mathbf{r}', \tau) \frac{\partial}{\partial \mathbf{R}_\nu} \hat{\mathbf{d}}(\mathbf{r}' - \hat{\mathbf{R}}_\nu, \tau) \right\rangle d\mathbf{r} d\mathbf{r}', \quad (\text{A2})$$

where $D(\mathbf{r} - \mathbf{r}', \tau) = \langle \hat{\mathbf{E}}(\mathbf{r}, 0) \hat{\mathbf{E}}^T(\mathbf{r}', \tau) \rangle$. This formula takes into account the finite value even of the smallest correlation time $\tau_c \sim 10^{-3}$ fs, which is due to the finite delocalization $r_A \sim 1$ Å of the dipole moment inside an atom. For the dipole moment, we can use a local approximation

$$\hat{\mathbf{d}}(\mathbf{r}' - \hat{\mathbf{R}}_\nu, \tau) = \hat{\mathbf{d}}_\nu(\tau) \delta(\mathbf{r}' - \hat{\mathbf{R}}_\nu - \hat{\mathbf{P}}_\nu \tau / m),$$

where $\hat{\mathbf{d}}_\nu(\tau)$ is the integrated internal dipole moment at the fixed point \mathbf{R}_ν at the moment τ ; $\hat{\mathbf{P}}_\nu$ is the translational momentum operator of the ν th atom with mass m . Then, in Eq. (A2) it is necessary to also take into account translational fluctuations due to the photon emission process, including interatomic correlations due to the exchange of photons between atoms.

To do that, we will first reveal the structure of the fluctuating force $\hat{\mathbf{F}}$. Switching to the Fourier representation, we find that the fluctuating force has the following form in the dipole approximation:

$$\hat{\mathbf{F}}_\tau = \int \sqrt{\frac{\hbar \omega}{4\pi^2}} \sum_\lambda \hat{\mathbf{d}}(t) \cdot \mathbf{e}_\lambda(\mathbf{k}) \times [\hat{a}_\lambda(\mathbf{k}) \exp(i\mathbf{k} \hat{\mathbf{R}}_\tau - i\omega t) - \text{h.c.}] i\mathbf{k} d\mathbf{k}, \quad (\text{A3})$$

where $\hat{a}_\lambda(\mathbf{k})$ are the photon annihilation operators and $\mathbf{e}_\lambda(\mathbf{k})$ are their polarization vectors. Then, for correlation matrix (A2), neglecting nonzero photon field temperature values and using the approximation $\hat{\mathbf{R}}_\tau = \hat{\mathbf{R}}_0 + \hat{\mathbf{v}}\tau$ for the translational motion, we get

$$G_{\mu\nu}(\tau) = \sum_s \mathcal{H}_s(\tau) \int \frac{\hbar \omega}{4\pi^2} \mathbf{d}_{\perp s}^\mu \cdot \mathbf{d}_{\perp s}^\nu \times \exp \left[i\omega \tau - \delta_{\mu\nu} \frac{\hbar k^2}{2m} \tau - i\mathbf{k}(\hat{\mathbf{R}}_{\mu\mu} + \hat{\mathbf{v}}_{\nu\mu} \tau) \right] \mathbf{k} \mathbf{k}^T d\mathbf{k}, \quad (\text{A4})$$

where $\hat{\mathbf{v}}$ is the atom velocity operator and \mathbf{d}_\perp is the transverse projection of the dipole moment onto the wave vector \mathbf{k} ; $\mathcal{H}_s(\tau) = \langle \sigma_{s\mu}^- \sigma_{s\nu}^+(\tau) \rangle$ is the correlation function of the s th transition operator. The factor $\delta_{\mu\nu}$ in Eq. (A4) shows that the corresponding contribution for different atoms does not affect the photon emission process, but the exchange of a photon between two atoms, i.e., a virtual emission-absorption interatomic process, happens without energy loss.

For the corresponding spectral intensity, we get

$$N_{\mu\nu}(\tilde{\omega}) = \int \sum_s S_s \left[\omega - \mathbf{k}\hat{\mathbf{v}}_{\nu\mu} - \delta_{\mu\nu} \frac{\hbar k^2}{2m} + \tilde{\omega} \right] \times \frac{\hbar\omega}{4\pi^2} \mathbf{d}_{\perp s}^{\mu} \cdot \mathbf{d}_{\perp s}^{\nu} \exp(-i\mathbf{k}\hat{\mathbf{R}}_{\nu\mu}) \mathbf{k}\mathbf{k}^T d\mathbf{k}, \quad (\text{A5})$$

where the matrix function S_s is the Fourier transformation of the internal atomic correlation function $\mathcal{H}_s(\tau)$. In order to calculate it, one has to calculate and apply the relaxation operator with the photon emission correlations taken into account in a similar way. In addition, the nonfluctuating coherent spectrum contribution has to be extracted, which means that the atomic transition operators are to be biased at their average value,

$$\hat{\sigma}_{\mu}^{\pm} \longrightarrow \Delta\hat{\sigma}_{\mu}^{\pm} = \hat{\sigma}_{\mu}^{\pm} - \langle \hat{\sigma}_{\mu}^{\pm} \rangle.$$

APPENDIX B

SELF-ACTION RDDI FORCE FLUCTUATIONS FOR A SINGLE ATOM

For a single atom reemitting photons, we can derive the fluorescence spectrum, which is simply the Fourier transformation of $\mathcal{H}_s(\tau)$, from Eq. (A5) at $\mu = \nu$ versus the frequency ω shifted due to the recoil momentum, which reads

$$N(\tilde{\omega}) = \frac{\hbar}{4\pi^2 c^5} \int \sum_s S_s \left[\omega \left(1 - \frac{\mathbf{n}\hat{\mathbf{v}}}{c} - \frac{\hbar\omega}{2mc^2} \right) + \tilde{\omega} \right] \times d_{\perp s}^2 \mathbf{nn}^T \omega^5 d\omega d\mathbf{n}. \quad (\text{B1})$$

From this equation, one can easily see that the spectrum of force fluctuations is an integral over the frequencies $\tilde{\omega}$ of emitted photons and their directions $\mathbf{n} = \mathbf{k}/k$, where the Doppler shift and recoil energy are taken into account. For integration over the velocities, we use here the Doppler broadened spectrum S_{D_s} instead of the spectrum S_s for a fixed atom.

Then, for the case of isotropic Doppler broadening, the fluorescence spectrum takes the form

$$N(\tilde{\omega}) = \frac{2}{15} \frac{\hbar}{\pi c^5} \int \sum_s d_s^2 S_{D_s} \left[\omega \left(1 - \frac{\hbar\omega}{2mc^2} \right) + \tilde{\omega} \right] \times \omega^5 d\omega (P_s^{\parallel} + 2P_s^{\perp}), \quad (\text{B2})$$

where P_s^{\parallel} , \parallel , $2P_s^{\perp}$ are the projection matrices onto the directions of the dipole moments and the orthogonal planes, respectively.

For simplicity, let us assume now that S_{D_s} can be treated as a narrow spectrum around the central frequency ω_s . Then, we should consider only the spectral range with $\tilde{\omega} \ll \omega_s$ and can neglect the recoil energy.

Using the integral equation $\int S_{D_s} d\omega = 2\pi n_s$, where n_s is the excited state population of the s th transition, which corresponds to the vanishing of $\tau \rightarrow 0$ in the correlation function $\hat{\sigma}_s^- \hat{\sigma}_s^+$, and replacing n_s with $n_s - \langle \hat{\sigma}_s^- \rangle \langle \hat{\sigma}_s^+ \rangle$ in order to extract the coherent part, we finally get

$$N(\omega) = \frac{\hbar^2}{5c^2} \sum_s \gamma_s \omega_s^2 (n_s - \langle \hat{\sigma}_s^- \rangle \langle \hat{\sigma}_s^+ \rangle) \times (P_s^{\parallel} + 2P_s^{\perp}), \quad (\text{B3})$$

where γ_s is the decay rate of the s th transition. From this formula, one can easily see that, at the low frequencies $\omega \ll \omega_s$, the spectral intensity of the force fluctuations does not depend on the frequency and, therefore, is simply white noise. Also, the spectral intensity is proportional to the emission rate of each transition and has an anisotropic character; i.e., the intensity of the components orthogonal to \mathbf{d}_s twofold exceeds the intensity of the parallel ones.

APPENDIX C

FORCE FLUCTUATIONS FOR TWO ATOMS INTERACTING VIA RDDI

For simplicity, let us assume that we can neglect the fluctuation frequencies $\tilde{\omega}$ with respect to the frequencies of emitted photons $\sim \omega_L$. Then, we can replace $G_{\mu\nu}(\tau)$ in Eq. (A4) with the delta function with respect to the time scale of interest, which means that we are interested only in calculating the integral value $N_{\mu\nu} = \int_{-\infty}^{\infty} G_{\mu\nu}(\tau) d\tau$. Inasmuch as the spectral width of the atomic emission fluctuations is narrow with respect to that of the vacuum field present in the integral of Eq. (A4), we can simply use the correlation function $\mathcal{H}_s(\tau) = \langle \sigma_{s\mu}^- \sigma_{s\mu}^+ \rangle \exp(-\omega_s t)$ and, neglecting the Doppler shift term for the same reason, get the following integral:

$$N_{\mu\nu} = \sum_s \frac{\hbar \omega_s^5 d_s^2}{2\pi c^5} \langle \Delta\sigma_{s\mu}^- \Delta\sigma_{s\nu}^+ \rangle \times \int \mathbf{e}_{\perp s}^{\mu} \cdot \mathbf{e}_{\perp s}^{\nu} \exp(-i\omega_s \mathbf{n}\hat{\mathbf{R}}_{\nu\mu}) \mathbf{nn}^T d\mathbf{n}. \quad (\text{C1})$$

The correlation $\langle \sigma_{s\mu}^- \sigma_{s\mu}^+ \rangle$ is nonzero because of the correlations due to photon exchange between the atoms that are represented by the corresponding terms in the multiatomic relaxation operator.

For the case in which the dipole moments are parallel to each other and orthogonal to the vector of displacement, i.e.,

$$\mathbf{e}_{\perp s}^{\mu} \parallel \mathbf{e}_{\perp s}^{\nu} \perp \mathbf{R}_{\mu\nu}, \quad (\text{C2})$$

the integral in Eq. (C1), which we will designate as I , can be expressed analytically in a simple way:

$$I = \pi \begin{pmatrix} I_1 & 0 & 0 \\ 0 & I_2 & 0 \\ 0 & 0 & I_3 \end{pmatrix}, \quad (C3)$$

with

$$\begin{aligned} I_1 &= \frac{4(9 - \varphi_{\mu\nu}^2) \cos \varphi_{\mu\nu}}{\varphi_{\mu\nu}^4} - \frac{4(9 - 4\varphi_{\mu\nu}^2) \sin \varphi_{\mu\nu}}{\varphi_{\mu\nu}^5}, \\ I_2 &= \frac{4(3 - \varphi_{\mu\nu}^2) \cos \varphi_{\mu\nu}}{\varphi_{\mu\nu}^4} - \frac{4(3 - 2\varphi_{\mu\nu}^2) \sin \varphi_{\mu\nu}}{\varphi_{\mu\nu}^5}, \\ I_3 &= \frac{-4(12 - 3\varphi_{\mu\nu}^2) \cos \varphi_{\mu\nu}}{\varphi_{\mu\nu}^4} \\ &\quad + \frac{4(12 - 7\varphi_{\mu\nu}^2 + \varphi_{\mu\nu}^4) \sin \varphi_{\mu\nu}}{\varphi_{\mu\nu}^5}, \end{aligned} \quad (C4)$$

where $\varphi_{\mu\nu} = \omega_s R_{\mu\nu}/c$ and the axes Z and X are set along $R_{\mu\nu}$ and the dipole moment, respectively.

At $R_{\mu\nu} \rightarrow 0$, i.e., in the case of a single atom, we get

$$I_2 = I_3 = 2I_1 = \frac{16}{15}, \quad (C5)$$

which is the same value that can be found by direct integration for a single atom. Fluctuations along the dipole moment are twofold weaker than in the orthogonal directions.

After calculation of the integral, Eq. (C1) is readily transformed into the following equation:

$$\begin{aligned} N_{\mu\nu} &= \frac{3\pi\hbar^2}{8c^2} \sum_s \gamma_s \omega_s^2 \langle \Delta\sigma_{s\mu}^- \Delta\sigma_{sv}^+ \rangle I \rightarrow \\ &\rightarrow \frac{\hbar^2}{5c^2} \sum_s \gamma_s \omega_s^2 \langle \Delta\sigma_{s\mu}^- \Delta\sigma_{sv}^+ \rangle (P_s^{\parallel} + 2P_s^{\perp}), \end{aligned} \quad (C6)$$

which differs from Eq. (B3) in that the term denoting single-atom dispersion is replaced with the interatomic correlation: $n_s - \langle \hat{\sigma}_s^- \rangle \langle \hat{\sigma}_s^+ \rangle \rightarrow \langle \Delta\sigma_{s\mu}^- \Delta\sigma_{sv}^+ \rangle$. From this equation, it also follows that the force fluctuations are correlated if there are correlations between incoherent oscillations of the atomic dipole transitions. In the limit of long-range interactions, we have

$$I_1 = I_2 = 0, \quad I_3 = \frac{4\varphi_{\mu\nu}}{\varphi_{\mu\nu}}, \quad (C7)$$

which means that the only long-range fluctuations are the fluctuations along the interatomic distance.

CALCULATION OF THE RADIATION RELAXATION OPERATOR OF THE TWO-ATOM ELECTRONIC SUBSYSTEM

We will start with the basic representation of the relaxation superoperator of a diffusion stochastic process in a form of the average second commutator [16]:

$$\begin{aligned} \mathcal{L} &= -\lim_{\Delta} \frac{1}{\hbar^2 \Delta} \iint_0^{\Delta} \left[\sum_k (\hat{\sigma}_k^+ \hat{\xi}_{k\tau_1}^- + \hat{\sigma}_k^- \hat{\xi}_{k\tau_1}^+), \right. \\ &\quad \left. \left[\sum_m (\hat{\sigma}_m^+ \hat{\xi}_{m\tau_2}^- + \hat{\sigma}_m^- \hat{\xi}_{m\tau_2}^+), \odot \right] \right] d\tau_1 d\tau_2, \end{aligned} \quad (D1)$$

$$\mathcal{L} = \sum \mathcal{L}_k + \sum_{k \neq m} \mathcal{L}_{km}, \quad (D2)$$

$$\begin{aligned} \mathcal{L}_{km} &= -\frac{\gamma_{kl}}{2} (\hat{\sigma}_k^- \hat{\sigma}_m^+ \odot + \odot \hat{\sigma}_k^- \hat{\sigma}_m^+ \\ &\quad - \hat{\sigma}_k^- \odot \hat{\sigma}_m^+ - \hat{\sigma}_m^- \odot \hat{\sigma}_k^+), \end{aligned} \quad (D3)$$

where the analog of the Lamb shift is omitted, and

$$\begin{aligned} \gamma_{kl} &= \lim_{\Delta} \frac{2}{\hbar^2 \Delta} \iint_0^{\Delta} \Re e \langle \hat{\xi}_{k\tau_1}^+ \hat{\xi}_{m\tau_2}^- \rangle d\tau_1 d\tau_2 \\ &= \int_{-\infty}^{\infty} \int \frac{\omega}{4\hbar\pi^2} \mathbf{d}_{\perp}^k \cdot \mathbf{d}_{\perp}^m \exp[i(\omega - \omega_a)\tau - i\mathbf{k}\hat{\mathbf{R}}_{km}] d\mathbf{k} d\tau \\ &= \frac{\omega_a^3}{2\pi\hbar c^3} \int \mathbf{d}_{\perp}^k \cdot \mathbf{d}_{\perp}^m \exp(-i\omega_a \mathbf{n}\hat{\mathbf{R}}_{km}/c) d\mathbf{n}. \end{aligned} \quad (D4)$$

For conditions (C2), it takes the form

$$\gamma_{kl} = \gamma_0 g, \quad g = \frac{3\varphi \cos \varphi - \sin \varphi + \varphi^2 \sin \varphi}{2\varphi^3}, \quad (D5)$$

where $\varphi = \omega_a R_{kl}/c$ and γ_0 is the single-atom decay rate.

For closely spaced atoms, we get simply $g = 1$, which corresponds to the total correlation of stationary excitations. Another extreme value, $g = -1$, corresponds to the case of antiparallel dipole moments \mathbf{d}_{μ} and \mathbf{d}_{ν} .

For large interatomic distances, we get

$$g = \frac{3 \sin \varphi}{2\varphi}. \quad (D6)$$

It is worthwhile to note here that the superposition of Eqs. (D6) and (C7) gives an inverse square dependence on the interatomic distance with the positive sign of the gI factor.

Relaxation operator (D3) without laser excitation can be simplified by introducing the symmetric and antisymmetric types of the dynamic variables with the

use of the basis ones of the types $\hat{e}_k \otimes \hat{e}_l \pm \hat{e}_l \otimes \hat{e}_k$. Then, for a two-level atom with a single-atom basis of dimension $n = 4$, we get 16 elements of the two-atom basis, consisting of four diagonal basis elements $\hat{e}_k \otimes \hat{e}_k$, six symmetric elements, and six antisymmetric elements. Because any physically feasible evolution operator always has zero matrix elements between the symmetric and antisymmetric subspaces, it can be reduced to the ten-dimensional space. In the general case of $g < 1$, the corresponding ten eigenvalues are listed below:

$$\lambda = \gamma_0 \left(0, -1 + g, -\frac{1+g}{2}, -\frac{1+g}{2}, -1, -1, -1 - g, -\frac{3+g}{2}, -\frac{3+g}{2}, -2 \right). \quad (\text{D7})$$

From this it follows that, for the closely spaced atoms, there are two independent stationary states, for $\lambda_0 = 0$ and $\lambda_1 = -1 + g = 0$, respectively. The eigen density matrix basis elements corresponding to the two eigenvalues λ_0 and λ_1 are given below:

$$\hat{\rho}_0 = \begin{pmatrix} 1 & 0 & 0 & 0 \\ 0 & 0 & 0 & 0 \\ 0 & 0 & 0 & 0 \\ 0 & 0 & 0 & 0 \end{pmatrix}, \quad \hat{\rho}_1 = \begin{pmatrix} -1 & 0 & 0 & 0 \\ 0 & 1/2 & -1/2 & 0 \\ 0 & -1/2 & 1/2 & 0 \\ 0 & 0 & 0 & 0 \end{pmatrix}. \quad (\text{D8})$$

Here, we have used the wavefunction basis $|00\rangle$, $|01\rangle$, $|10\rangle$, $|11\rangle$, where the indices 0 and 1 denote the ground and excited states of the atoms, respectively. The first matrix corresponds to the two-atomic vacuum state, while the second one corresponds to the sum of the density matrix of the ground state $|00\rangle$ (with the negative sign) and the coherent antisymmetric excitation of both

atoms. The corresponding eigenbasis \hat{e}_k of the physical variables has an identity matrix equal to the null eigenvector and the matrix

$$\hat{e}_1 = \begin{pmatrix} 0 & 0 & 0 & 0 \\ 0 & 1/2 & -1/2 & 0 \\ 0 & -1/2 & 1/2 & 0 \\ 0 & 0 & 0 & \frac{1-g}{1+g} \end{pmatrix} \quad (\text{D9})$$

corresponding to the $1 - g$ eigenvalue. The null eigenvector represents an antisymmetric coherent excitation with the population $(1 - g)/(1 + g)$ of the excited state.

In order to calculate the force fluctuations, we have to first investigate the null-space problem for the relaxation operator in the presence of laser excitation. Within the frame of the rotation wave approximation (RWA), when the unperturbed dynamics is present with free precession with the laser frequency ω_L , the corresponding contribution to the total Liouvillian is

$$\mathcal{L}_L = i \sum_{\mu} \frac{g_{L\mu}}{2} [\hat{\sigma}_{1\mu}, \odot] - i \sum_{\mu} \frac{\delta}{2} [\hat{\sigma}_{3\mu}, \odot], \quad (\text{D10})$$

where $\hat{\sigma}_{1\mu}$ and $\hat{\sigma}_{3\mu}$ are the Pauli matrices for the μ th atom, $g_{L\mu}$ is the corresponding Rabi frequency, and δ is the laser detuning. For simplicity, we neglect here the nonradiative dipole-dipole interaction.

For specific geometry (C2), we have $g_{L\mu} = g_L$ and, using the ten-dimensional representation of the total operator $\mathcal{L} = \mathcal{L}_r + \mathcal{L}_L$, we can then calculate its eigenvalues and the stationary null-space vector. The corresponding stationary density matrix has the form

$$\hat{\rho} = \begin{pmatrix} \frac{A_1}{A_0} & \frac{\tilde{g}_L(i + 2\tilde{\delta})A_2}{A_0} & \frac{\tilde{g}_L(2\tilde{\delta} + i)A_2}{A_0} & \frac{\tilde{g}_R^2(2\tilde{\delta} + i)(2\tilde{\delta} + i + ig)}{A_0} \\ \frac{\tilde{g}_L(2\tilde{\delta} - i)A_2^*}{A_0} & \frac{\tilde{g}_L^2(1 + 4\tilde{\delta}^2 + \tilde{g}_L^2)}{A_0} & \frac{\tilde{g}_L^2(1 + 4\tilde{\delta}^2)}{A_0} & \frac{\tilde{g}_L^3(2\tilde{\delta} + i)}{A_0} \\ \frac{\tilde{g}_L(2\tilde{\delta} - i)A_2^*}{A_0} & \frac{\tilde{g}_L^2(1 + 4\tilde{\delta}^2)}{A_0} & \frac{\tilde{g}_L^2(1 + 4\tilde{\delta}^2 + \tilde{g}_L^2)}{A_0} & \frac{\tilde{g}_L^3(2\tilde{\delta} + i)}{A_0} \\ \frac{\tilde{g}_L^2(2\tilde{\delta} - i)(2\tilde{\delta} - i - ig)}{A_0} & \frac{\tilde{g}_L^3(2\tilde{\delta} - i)}{A_0} & \frac{\tilde{g}_L^3(2\tilde{\delta} - i)}{A_0} & \frac{\tilde{g}_L^4}{A_0} \end{pmatrix}, \quad (\text{D11})$$

where

$$A_0 = (1 + g)^2 + 4(\tilde{g}_L^2 + \tilde{\delta}^2) + 4(1 + g)^2\tilde{\delta}^2 + 4(\tilde{g}_L^2 + 2\tilde{\delta}^2)^2,$$

$$A_1 = (1 + g)^2 + 2(\tilde{g}_L^2 + 2\tilde{\delta}^2) + 4(1 + g)^2\tilde{\delta}^2 + (\tilde{g}_L^2 + 4\tilde{\delta}^2)^2,$$

$$A_2 = 1 + 4\tilde{\delta}^2 + g + 2i\tilde{\delta}g + \tilde{g}_L^2,$$

and $\tilde{g}_L = g_L/\gamma_0$, $\tilde{\delta} = \delta/\gamma_0$.

With the help of Eqs. (D11), we can calculate the normalized correlation coefficient $\kappa = N_{12}/N_{11}$:

$$\kappa = \frac{N_{12}}{N_{11}} = \frac{-2g(1+4\delta^2)}{A_3}, \quad (\text{D12})$$

where

$$N_{11} \propto \langle \Delta\sigma_\mu^- \Delta\sigma_\mu^+ \rangle = \frac{2g_L^4 A_3}{A_0^2},$$

$$A_3 = [1 + 2(g_L^2 + 2\delta^2)]^2 + g^2(1 + 4\delta^2).$$

From Eq. (D12) it follows that the correlation effects are mostly revealed in the weak-field limit, at $\mathbf{E}_L \mathbf{d}_\mu / \hbar \ll \gamma$, i.e., at the extreme values of $\kappa = \mp 1$, which correspond to the values of $g = \pm 1$ and $\delta = 0$.

With the help of two-atom density matrix (D11), one can calculate any characteristic of the internal atomic dynamics, including the correlation matrix $\mathcal{H}_s(\tau) = \langle \sigma_{s\mu}^- \sigma_{s\mu}^+ \rangle \exp(-\omega_s t)$, which is used to determine force correlation matrix (A4).

REFERENCES

1. *The Physics of Quantum Information: Quantum Cryptography, Quantum Teleportation, Quantum Computation*, Ed. by D. Bouwmeester, A. Ekert, and A. Zeilinger (Springer-Verlag, New York, 2000).
2. R. Grimm, M. Weidemüller, and Y. B. Ovchinnikov, *Adv. Atom. Mol. Opt. Phys.* **42**, 95 (2000).
3. N. Schlosser, G. Reymond, I. Protsenko, and P. Grangier, *Nature* **411**, 1024 (2001).
4. D. Schrader, S. Kuhr, W. Alt, *et al.*, *Appl. Phys.* **B73**, 819 (2001).
5. B. Ueberholz, S. Kuhr, D. Frese, *et al.*, *J. Phys.* **B33**, 4 (2000).
6. D. N. Yanyshev, B. A. Grishanin, and V. N. Zadkov, *SPIE Procs.* **4750**, 104 (2002).
7. J. Weiner, V. S. Bagnato, S. Zilio, and P. S. Julienne, *Rev. Mod. Phys.* **71**, 1 (1999).
8. E. L. Raab, M. Prentiss, A. Cable, *et al.*, *Phys. Rev. Lett.* **59**, 2631 (1987).
9. D. Frese, B. Ueberholz, S. Kuhr, *et al.*, *Phys. Rev. Lett.* **85**, 3777 (2000).
10. M. Ben Dahan, E. Peik, J. Reichel, *et al.*, *Phys. Rev. Lett.* **76**, 4508 (1996).
11. H. Wallis, *Phys. Rep.* **255**, 203 (1995).
12. M. Lax, *Fluctuation and Coherence Phenomena in Classical and Quantum Physics* (Gordon Breach, New York, 1968).
13. L. Mandel and E. Wolf, *Optical Coherence and Quantum Optics* (Cambridge Univ. Press, Cambridge, 1995; Fizmatlit, Moscow, 2000).
14. A. M. Bonch-Bruевич, S. G. Przhibel'ski, V. V. Khromov, and S. I. Yakovlenko, *Byull. Akad. Nauk. SSSR*, **48** (3), 587 (1984).
15. B. A. Grishanin, *Quantum Electrodynamics for Radiophysicists* (Mosk. Gos. Univ., Moscow, 1981) [In Russian].
16. B. A. Grishanin, <http://comsim1.phys.msu.ru/people/grishanin/teaching/qsp/>.

SPELL: 1. inneighboring